# Development of a Modular Cryo-Transfer Station for the Side-Entry Transmission Electron Microscope<sup>†</sup>

Alexander Reifsnyder<sup>1,\*,‡</sup>, Jordan A. Hachtel<sup>2,§</sup>, Andrew R. Lupini<sup>2,§</sup>, and David W. McComb<sup>1,3,‡</sup>

#### **Abstract**

Cryo-transfer stations are essential tools in the field of cryo-electron microscopy, enabling the safe transfer of frozen vitreous samples between different stages of the workflow. However, existing cryo-transfer stations are typically configured for only the two most popular sample holder geometries and are not commercially available for all electron microscopes. Additionally, they are expensive and difficult to customize, which limits their accessibility and adaptability for research laboratories. Here, we present a new modular cryo-transfer station that addresses these limitations. The station is composed entirely of 3D-printed and off the shelf parts, allowing it to be reconfigured to a fit variety of microscopes and experimental protocols. We describe the design and construction of the station and report on the results of testing the cryo-transfer station, including its ability to maintain cryogenic temperatures and transfer frozen vitreous samples as demonstrated by vibrational spectroscopy. Our findings demonstrate that the cryo-transfer station performs comparably to existing commercial models, while offering greater accessibility and customizability. The design for the station is open source to encourage other groups to replicate and build on this development. We hope that this project will increase access to cryo-transfer stations for researchers in a variety of disciplines with nonstandard equipment.

Key words: 3D printing, CAD, cryo-transfer, EELS, ice, open source, TEM, vibrational spectroscopy, vitreous

#### Introduction

The transmission electron microscope (TEM) is one of the most versatile tools in characterization. TEM imaging allows direct observation of the sample at high spatial resolution, and it can be augmented with additional detectors to collect data of many types at higher spatial resolution than can be achieved with other techniques. However, not all samples can be studied in the TEM at room temperature. Organic and biological samples often need to be studied at cryogenic temperatures to reduce beam damage, preserve delicate structures, and examine the material in a natural hydrated state (Taylor & Glaeser, 1976; Dubochet et al., 1982; Jasim et al., 2021).

For such materials, a frozen hydrated sample must be prepared outside the microscope, normally using a specialized plunge freezer. Aqueous samples are rapidly frozen to form amorphous/vitreous ice, which preserves the microstructure of the sample and generates fewer imaging artifacts than crystalline ice (Stewart, 1989). The samples must then be loaded into the microscope without warming up and devitrifying the ice. The samples must also be protected from frost formation due to humidity in the air, which would render the sample

too thick for TEM. A cryo-transfer station protects the specimen as it is loaded into the sample holder. A sliding shutter or other means of encapsulating the sample prevents frost formation during the transfer from the cryo-transfer station to the TEM (Frederik & Busing, 1986).

Developments in microscope design have enabled some manufacturers to reach extremely high energy resolutions, up to 3 meV. The Nion HERMES STEM can reach <6 meV energy resolution at 60 kV, allowing observation of the vibrational loss regime (Dellby et al., 2023, 2020). Vibrational excitations in electron energy-loss spectroscopy (EELS), typically observed in the range 0–500 meV, can potentially yield highly detailed bonding information with atomic-scale spatial resolution (Dwyer et al., 2016; Crozier, 2017; Hachtel et al., 2019; Krivanek et al., 2019). Samples which require cryo-transfer have not yet been studied with vibrational spectroscopy in the electron microscope because cryo-transfer systems, composed of a sample rod and transfer station, are not available for every TEM manufacturer, and they are not designed to be modified by the user.

There is currently no commercially available cryo-transfer system for a Nion side-entry microscope, which uses a proprietary sample holder geometry. It is possible to adapt a

<sup>&</sup>lt;sup>1</sup>Department of Materials Science and Engineering, Fontana Laboratories Suite 2136, 140 W. 19th Avenue, Columbus, OH 43210, USA

<sup>&</sup>lt;sup>2</sup>Center for Nanophase Materials Sciences, Oak Ridge National Laboratory, 1 Bethel Valley Road, Oak Ridge, TN 37830, USA

<sup>&</sup>lt;sup>3</sup>Center for Electron Microscopy and Analysis, 1305 Kinnear Rd Suite 100, Columbus, OH 43212, USA

<sup>\*</sup>Corresponding author: Alexander Reifsnyder, E-mail: Reifsnyder.3@osu.edu

<sup>&</sup>lt;sup>†</sup>Notice: This manuscript has been authored by UT-Battelle, LLC, under contract no. DE-AC05000R22725 with the US Department of Energy. The United States Government retains and the publisher, by accepting the article for publication, acknowledges that the United States Government retains a non-exclusive, paid-up, irrevocable, world-wide license to publish or reproduce the published form of this manuscript, or allow others to do so, for the United States Government purposes. The Department of Energy will provide public access to these results of federally sponsored research in accordance with the DOE Public Access Plan (http://energy.gov/downloads/doe-public-access-plan).

<sup>&</sup>lt;sup>‡</sup>Current address: Department of Materials Science and Engineering, Fontana Laboratories Suite 2136, 140 W. 19th Avenue, Columbus, OH 43210.

<sup>&</sup>lt;sup>5</sup>Current address: Center for Nanophase Materials Sciences, Oak Ridge National Laboratory, 1 Bethel Valley Road, Oak Ridge, TN 37830.

Alexander Reifsnyder et al. 725

cryo-transfer holder that is available in a ThermoFisher-compatible geometry, like the Gatan Elsa cryo-transfer holder, with a sleeve to increase the diameter and add the appropriate airlock interfaces. However, once this adapter is installed it will no longer fit in the original cryo-transfer station, making cryo-transfer impossible. In this project we designed, constructed, and tested a modular cryo-transfer station which works with a Nion-compatible side-entry sample holder and could be adjusted to fit other airlock designs. The development of this capability enables EELS to be performed on frozen hydrated samples with unprecedented energy resolution.

#### **Materials and Methods**

To ensure a safe transfer of a sample in vitreous ice, the transfer station needs to reach and maintain a safe transfer temperature of 143 K (Dubochet et al., 1982). Additionally, the Nion adapter sleeve has a front sealing surface which mates with an internal o-ring inside the microscope, as shown in Figure 1. All of the printed parts have been optimized for use with a desktop-style FDM 3D printer.

#### **Holder Construction**

It is critical that no frost forms on the sealing surface at the sample end of the Nion adapter sleeve during sample transfer, as this could interrupt the internal o-ring seal in the microscope and vent or contaminate the UHV environment inside the microscope column. To prevent frost formation, the temperature of the Nion adapter sleeve must be maintained at or near room temperature while the tip of the sample rod must be maintained at or below 143 K to prevent accidental devitrification of the sample.

Figure 2 presents a labeled CAD rendering of the cryotransfer station (CTS), which was designed for use with Nion-compatible side-entry sample holders. This prototype has several design choices which deviate from the Gatan (OEM) station which shipped with the Elsa holder, which was designed for use with ThermoFisher-compatible sample rods.

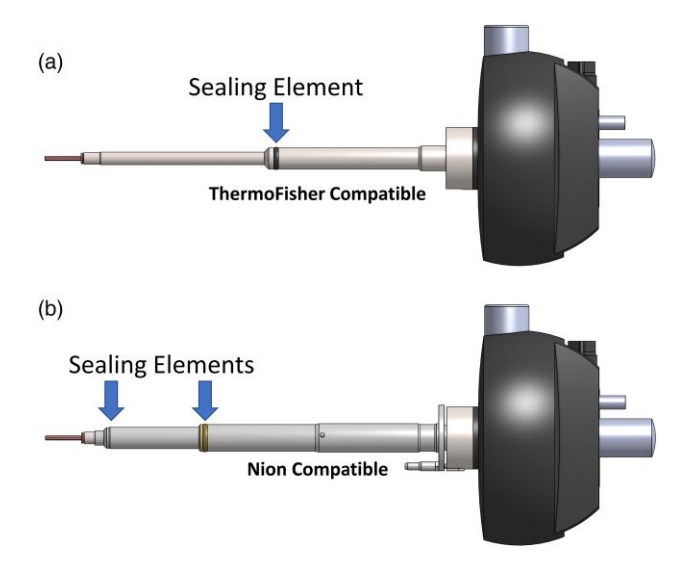


**Fig. 1.** A ThermoFisher-compatible Gatan Elsa cryo-transfer sample holder without (**a**) and with (**b**) a Nion side-entry adapter installed.

The prototype has a sliding carriage which is used to hold the sample rod and slide it into place. The OEM station has a long tube which the holder is inserted into, providing the support of the rod, positioning guidance, interfacing with the dewar, and o-ring sealing. The CTS has separated these features into two distinct parts. The sliding carriage of the CTS provides support of the rod and positioning guidance, while the transfer tube interfaces with the dewar and provides an o-ring seal. The sliding carriage was added to minimize contact of 3D-printed parts with the portion of the sample rod which is exposed to UHV inside the microscope, thereby reducing potential for contamination introduced during the transfer process.

The transfer tube of the CTS, shown in Figure 3, is significantly shorter than the OEM station, due in part to the different o-ring positions of the Nion adapter sleeve compared to the ThermoFisher-compatible sample rods. However, the main purpose of the OEM tube is to support the rod, which is not required in the CTS. The transfer tube of the CTS prevents the Nion adapter sleeve from becoming too cold and developing frost on the front sealing surface. This function is accomplished by limiting the amount of cold air from the dewar that can enter the transfer tube.

Despite these precautions, initial tests indicated that frost could form on the front sealing surface of the Nion adapter sleeve, as shown in Figure 4. Solid transfer tubes, even those with minimal clearance around the rod to limit ingress of cold air from the dewar, quickly generated frost on the front of the sample rod. To provide additional protection from excessive cooling of the Nion adapter sleeve, the transfer tube was redesigned to accept room temperature gas flowing though as a warming medium. Designs of the transfer tube which injected laminar streams of gas directly along the outer surface of the adapter sleeve were found to prevent frost formation, but the continuous supply of warm gas entering the transfer dewar interfered with the system's ability to reach and maintain a safe transfer temperature. Similarly, designs with a helical gas flow in contact with the holder appeared to perform better, but also interfered. To prevent frost formation without the gas entering the transfer dewar, the tube was redesigned to accommodate helical channels which carry room temperature gas through the body of the transfer tube. These channels, seen in Figure 3 between the inner and outer diameter of the transfer tube, do not allow direct contact of gas with the sample rod body. This provides the additional benefit that any source of room temperature gas may be used without regard to oil, dust, or water content. The room temperature gas flowing through the channels continuously limits the amount of cooling experienced by the adapter sleeve by acting as a heat exchanger with the cold air inside the transfer tube. Used gas exits outside the dewar to prevent unnecessary warming of the sample dewar. As shown in Figure 4, this heat exchanger design reached a safe transfer temperature while preventing the formation of frost on the front sealing surface of the adapter sleeve for over 30 min.

## Sample Preparation

To test the performance of the CTS, a sample of vitreous ice was prepared. Vitreous ice will devitrify rapidly above 143 K, the chosen safe transfer limit for the CTS (Dubochet et al., 1982). A Pelco 200 mesh gold grid with lacey carbon support film was processed with air in a glow discharge system

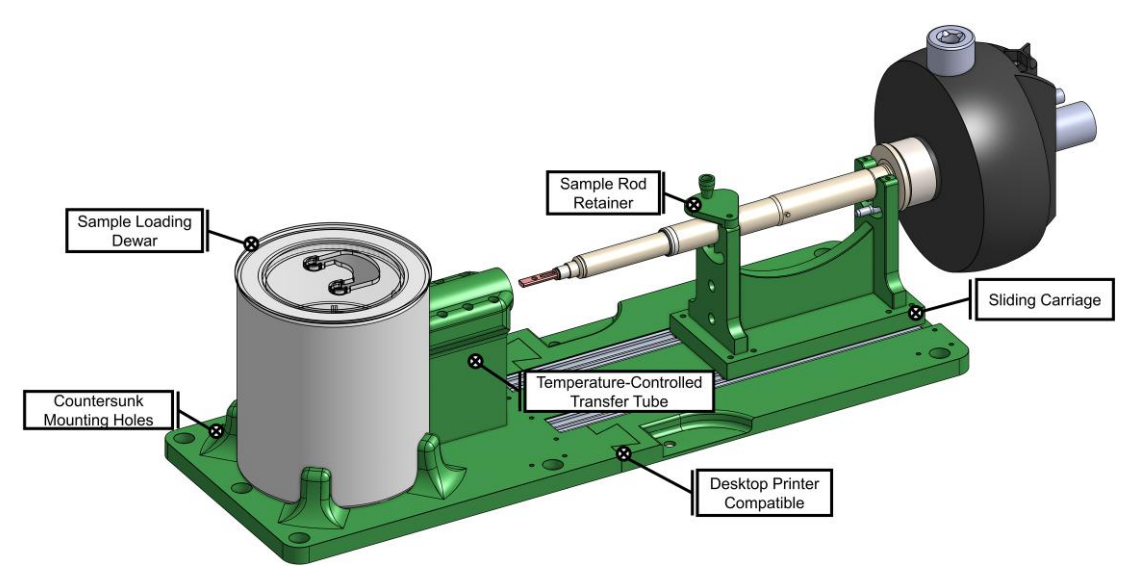
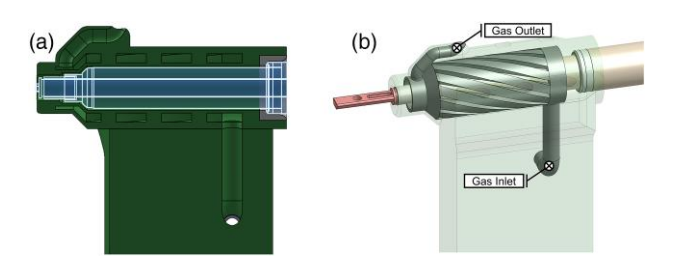


Fig. 2. CAD rendering of the assembled cryo-transfer station.



**Fig. 3.** Detail views of how the transfer tube interacts with the sample rod (a) and with the helical heat transfer channels highlighted (b).

to make the support film hydrophilic. A thin film of distilled water was added to the grid with a ThermoFisher Scientific VitroBot, before flash freezing in liquid ethane. Sample preparation took place approximately 2 h before loading the sample into the Elsa holder. The samples were stored under liquid nitrogen during this time to prevent devitrification. Compressed UHP nitrogen gas was used for the heat exchanger, attached to a needle valve to control flow rate. As discussed above, any gas source may be used for the transfer tube, and compressed nitrogen was selected for convenience.

## Results

After the sample was successfully transferred into the microscope, vibrational EELS data was collected, presented in Figure 5. The spectrum shows a distinct peak at ~420 meV due to the O-H stretch. After collecting data on the amorphous sample, the Elsa holder was programmed to heat up to 160 K to devitrify the sample before cooling back down to 103 K for further analysis. The samples were held at or above 160 K for approximately 5 min. After heating, the relative intensity of the O-H stretch peak has increased significantly, but more importantly we can see that lineshape has changed as well. The amorphous ice peak is symmetric about the common O-H stretch frequency of ~420 meV (418 meV observed), while the recrystallized ice peak is asymmetric in the lowenergy side and is now peaks at 413 meV. Moreover, while subtle bands of vibration are visible even in the amorphous ice at 109, 203, and 284 meV, these modes become more

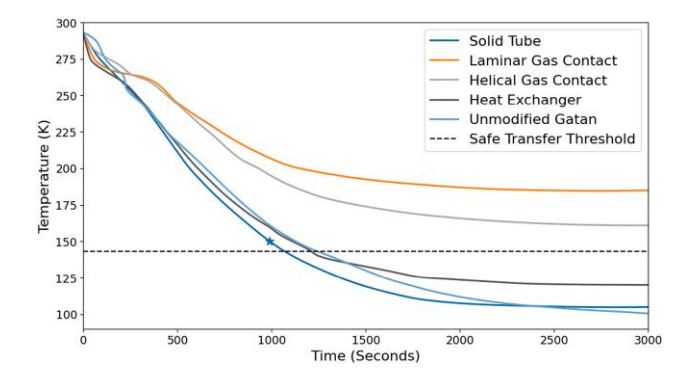


**Fig. 4.** A graph of the temperature performance of different transfer tube designs. A star indicates the point where frost formation was first observed in the solid tube design (dark blue line). Designs where the room temperature gas was in contact with the sleeve (orange and light gray lines) did not achieve a safe transfer temperature (dotted horizontal line)

pronounced and slightly shifted to 110, 201, and 280 meV after recrystallizing. Based upon previous research from the Cryo-EM community, it is predicted that these changes arise from the emergence of ice IC, a cubic form of ice known to form upon devitrification of samples flash frozen in ethane (Dubochet et al., 1982). These observations are consistent with published measurements with vibrational EELS and FTIR comparing vitreous ice to ice IC (Hardin & Harvey, 1973; Krivanek et al., 2019; Li et al., 2021).

#### **File Distribution**

The source files for project have been released to the public under the Creative Commons Attribution, Share Alike 4.0 license. Please read the license details at <a href="https://creativecommons.org/licenses/by-sa/4.0/">https://creativecommons.org/licenses/by-sa/4.0/</a>. The files can be retrieved from <a href="https://github.com/AlexanderReifsnyder/ModularCryoTransferStation">https://github.com/AlexanderReifsnyder/ModularCryoTransferStation</a>. The design is currently on Version 1. This repository contains two folders for each version. One is pre-exported STLs, ready to print and use immediately. The other contains the SLDPRT source files for users who to modify the design to suit their specific needs. Each version

Alexander Reifsnyder et al. 727

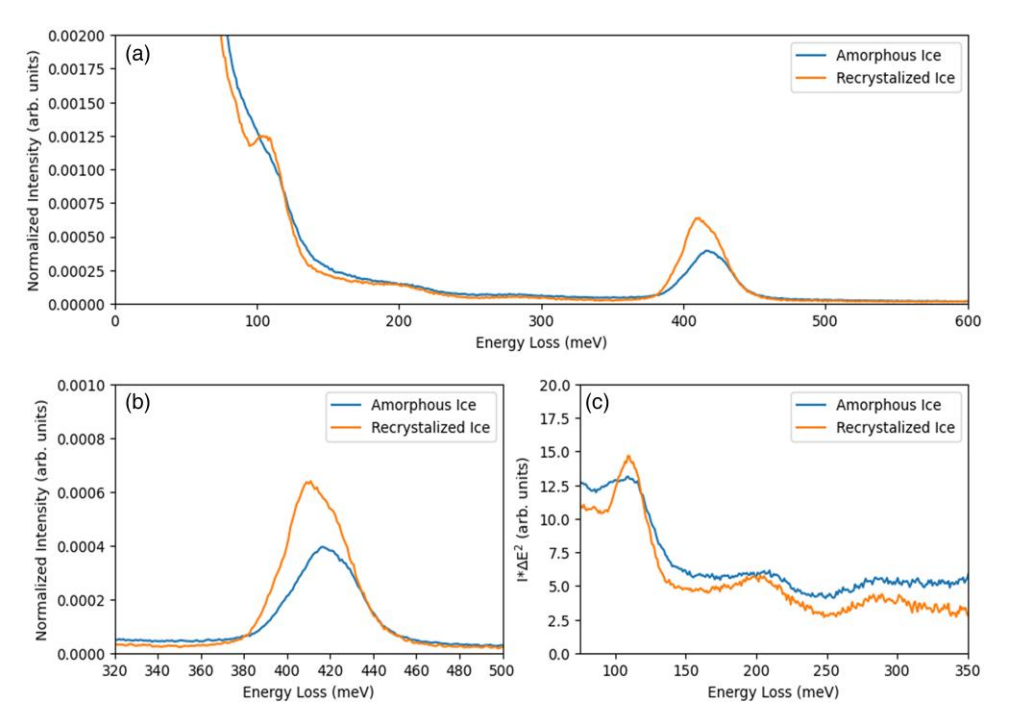


**Fig. 5.** The vibrational EELS spectrum of an ice sample before and after intentional devitrification. (a) shows the full vibrational spectrum while the lower panels highlight the change in the (b) 420 meV O-H stretch plotted on a normalized scale and (c) lower energy librations and stretching modes plotted with Intensity \* Energy-Loss Squared y-axis scaling.

also contains a bill of materials with links to the products used in the CTS prototype.

#### Conclusion

This study has detailed the development of a 3D printable cryo-transfer station for use with nonstandard side-entry sample holders. Initial transfer tests using vitreous ice have been presented, which have demonstrated the transfer station's ability to prevent devitrification of a sample during the loading process. The source files of the project have been made available with an opensource license to allow anyone to replicate and build on this project. Ongoing improvements are planned for the CTS, most importantly developing a 3D printed or traditionally machined dewar insert to replace the OEM insert which was used for the tests. A beta-testing version is included in the file repository, but it has not been extensively tested to ensure safe transfer.

All designs included in the file repository are parametric, allowing those with access to CAD software to easily modify the dimensions and features of each module, or design new modules to fit a specific requirement. While the station was configured for a Nion-compatible side-entry holder for this study, reconfiguring the modules for a different holder design is fast and easy. Switching just four parts (in three modules) of the station would allow a different diameter holder to be used, and only one additional part would need to be modified if the holder was longer than a Nion-style holder. This adaptability is a key feature of this project, demonstrating a framework to make customized cryo-transfer station for nonstandard airlock geometries. Additionally, any experiment which might otherwise require modifying the cryo-transfer station would be able to design their own cryo-transfer station to meet the needs of the experiment, using this project as a base or a template as needed.

# **Availability of Data and Materials**

The authors have declared that no datasets apply for this piece.

# **Acknowledgments**

All 3D printing and EELS measurements were completed as part of a user proposal at the Center for Nanophase Materials Sciences, which is a US Department of Energy, Office of Science User Facility using instrumentation within ORNL's Materials Characterization Core provided by UT-Battelle, LLC, under contract no. DE-AC05-00OR22725 with the DOE and sponsored by the Laboratory Directed Research and Development Program of Oak Ridge National Laboratory, managed by UT-Battelle, LLC, for the US Department of Energy. Additional support was provided by the US Department of Energy, Office of Basic Energy Sciences (DOE-BES), Division of Materials Sciences and Engineering under contract ERKCS89.

# Financial Support

This research was supported by the Center for Emergent Materials, an NSF MRSEC, under award number DMR-2011876.

### **Conflict of Interest**

The authors declare that they have no competing interest.

#### References

Crozier PA (2017). Vibrational and valence aloof beam EELS: A potential tool for nondestructive characterization of nanoparticle surfaces. *Ultramicroscopy* **180**, 104–114. https://doi.org/10.1016/j.ultramic.2017.03.011

- Dellby N, Lovejoy T, Corbin G, Johnson N, Hayner R, Hoffman M, Hrncrik P, Plotkin-Swing B, Taylor D & Krivanek O (2020). Ultra-high energy resolution EELS. *Microsc Microanal* 26, 1804–1805. https://doi.org/10.1017/S1431927620019406
- Dellby N, Quillin SC, Krivanek OL, Hrncirik P, Mittelberger A, Plotkin-Swing B & Lovejoy TC (2023). Ultra-high resolution EELS analysis and STEM imaging at 20 keV. *Microsc Microanal* 29, 626–627. https://doi.org/10.1093/micmic/ozad067.305
- Dubochet J, Lepault J, Freeman R, Berriman JA & Homo J-C (1982). Electron microscopy of frozen water and aqueous solutions. *J Microsc* 128, 219–237. https://doi.org/10.1111/j.1365-2818.1982.tb04625.x
- Dwyer C, Aoki T, Rez P, Chang SLY, Lovejoy TC & Krivanek OL (2016). Electron-beam mapping of vibrational modes with nanometer spatial resolution. *Phys Rev Lett* 117, 256101. https://doi.org/10.1103/PhysRevLett.117.256101
- Frederik PM & Busing WM (1986). Cryo-transfer revised. *J Microsc* 144, 215–221. https://doi.org/10.1111/j.1365-2818.1986.tb02802.x
- Hachtel JA, Huang J, Popovs I, Jansone-Popova S, Keum JK, Jakowski J, Lovejoy TC, Dellby N, Krivanek OL & Idrobo JC (2019). Identification of site-specific isotopic labels by vibrational spectroscopy in the electron microscope. *Science* 363, 525–528. https://doi.org/10.1126/science.aav5845
- Hardin AH & Harvey KB (1973). Temperature dependences of the ice I hydrogen bond spectral shifts—I: The vitreous to cubic ice I phase

- transformation. Spectrochim Acta A Mol Biomol Spectrosc 29, 1139–1151. https://doi.org/10.1016/0584-8539(73)80152-7
- Jasim AM, He X, Xing Y, White TA & Young MJ (2021). Cryo-ePDF: Overcoming electron beam damage to study the local atomic structure of amorphous ALD aluminum oxide thin films within a TEM. ACS Omega 6, 8986–9000. https://doi.org/10.1021/ acsomega.0c06124
- Krivanek OL, Dellby N, Hachtel JA, Idrobo J-C, Hotz MT, Plotkin-Swing B, Bacon NJ, Bleloch AL, Corbin GJ, Hoffman MV, Meyer CE & Lovejoy TC (2019). Progress in Ultrahigh Energy Resolution EELS. 75th Birthday of Christian Colliex, 85th Birthday of Archie Howie, and 75th Birthday of Hannes Lichtel PICO 2019—Fifth Conference on Frontiers of Aberration Corrected Electron Microscopy 203, 60–67.
- Li H, Karina A, Ladd-Parada M, Späh A, Perakis F, Benmore C & Amann-Winkel K (2021). Long-range structures of amorphous solid water. J Phys Chem B 125, 13320–13328. https://doi.org/10.1021/ acs.jpcb.1c06899
- Stewart M (1989). Transmission electron microscopy of frozen hydrated biological material. *Electron Microsc Rev* 2, 117–121. https://doi.org/10.1016/0892-0354(89)90012-9
- Taylor KA & Glaeser RM (1976). Electron microscopy of frozen hydrated biological specimens. *J Ultrastruct Res* 55, 448–456. https://doi.org/10.1016/S0022-5320(76)80099-8